Frost growth and densification on a flat surface in laminar flow with variable humidity

M. Kandula[1]

ESC - Team QNA, NASA Kennedy Space Center, Florida 32899, USA

Abstract

Experiments are performed concerning frost growth and densification in laminar flow over a flat surface under conditions of constant and variable humidity. The flat plate test specimen is made of aluminum-6031, and has dimensions of 0.3 mx0.3 mx6.35 mm. Results for the first variable humidity case are obtained for a plate temperature of 255.4 K, air velocity of 1.77 m/s, air temperature of 295.1 K, and a relative humidity continuously ranging from 81 to 54%. The second variable humidity test case corresponds to plate temperature of 255.4 K, air velocity of 2.44 m/s, air temperature of 291.8 K, and a relative humidity ranging from 66 to 59%. Results for the constant humidity case are obtained for a plate temperature of 263.7 K, air velocity of 1.7 m/s, air temperature of 295 K, and a relative humidity of 71.6 %. Comparisons of the data with the author's frost model extended to accommodate variable humidity suggest satisfactory agreement between the theory and the data for both constant and variable humidity.

Key words: Frost growth, Densification, Variable humidity, Flat Surface, Laminar flow

E-mail: max.kandula-1@nasa.gov

Nomenclature

h_c convective heat transfer coefficient (W/m^2 K)

h_m convective mass transfer coefficient (kg/m^2 s)

k_f effective thermal conductivity of frost (W/m K)

L plate length (m)

L_{sv} latent heat of sublimation (kJ/kg)

T temperature (K)

u air velocity (m/s)

Greek Symbols

ϕ relative humidity (%)

ν kinematic viscosity (m^2/s)

ρ_f frost density (kg/m^3)

ρ_{ice} ice density (kg/m^3)

ω humidity ratio of moist air, kg (water vapor)/kg(dry air) or kg_v/kg_a

Subscripts

a air

m melting

s frost surface

v water vapor

w wall

1. Introduction

Frost formation represents an important consideration in many areas of modern technology such as cryogenics, refrigeration, aerospace, meteorology and various process industries (gas coolers, refrigerators, regenerators, freeze-out purification of gases, cryopumping, and the storage of cryogenic liquids).

Experimental studies for frost formation on flat surfaces were published by various investigators; see Jones and Parker [1], Yonko and Sepsy [2], Östin and Anderson [3], Lee et al. [4,5], Cheng and Wu [6], and Hermes et al. [7] among others. Experiments by Östin and Anderson [3] and others suggest that the frost growth depends strongly on the cold plate temperature and the air humidity.

Most of the existing data correspond to constant air humidity, excepting the data of Jones and Parker [1] which consider only a discontinuous change in air humidity. In important practical situations, especially in cryogenic storage and launch vehicle applications, the boundary circumstances involve variable humidity as well as variable surface temperature. Frost data for a continuous variation of humidity or surface temperature even on relatively simple geometries such as flat surfaces appear to be lacking in the literature. The validation of theoretical models remains difficult in the absence of such experimental data.

It is the objective of this work to report experimental data for frost growth and densification on a flat horizontal surface in laminar flow under conditions of variable humidity, but at constant wall temperature. In this connection, the recent frost model by the author [8], which was validated with existing data for constant humidity, will be extended to the case of variable humidity. This extended model will then be validated by a comparison of the present data on flat surfaces for variable humidity as well as constant humidity.

2. Description of the Experimental Setup

A brief description of the experimental setup is presented as follows. **Fig.** 1 shows a schematic of the experimental setup. The test specimen consists of a square flat plate made of aluminum-6031, and has dimensions of 0.3 m x 0.3m x 6.35 mm. It forms a central and integral part of a larger plate of dimensions 0.6 m x 0.6m x 6.35 mm. The aluminum surface is hydrophylic, and has a surface roughness range of about 0.8-3.2 μ m. The surface condition (such as surface roughness and wetting condition) affects the nucleation density of the frost formation which directly influences the frost porosity, density and height.

Figure. 2a shows a photographic view of the test facility. The test plate is cooled by liquid nitrogen which flows from LN2 dewar (storage tank), while the rest of the plate surrounding the test section is insulated with aerogel insulation. The control temperature of the plate is measured by a thermocouple placed underneath the plate surface, and the flow rate necessary to achieve a

given plate temperature is adjusted by a solenoid valve. The uncertainty in the thermocouple temperature is ± 0.6 K.

The air flow is provided by a large fan placed upstream of the plate leading edge. It is recognized that a household blower cannot precisely control the air flow speed right on the cold plate as air flows from all directions in a room. In the experiments, the fan necessarily produced unsteadiness in the flow velocity unlike in the case of a wind tunnel where flow steadiness can be assured. Under these circumstances, which are expected near the launch pad, an average air velocity is considered representative of the test conditions. The air velocity is measured with a Young Model 85000 Ultrasonic Anemometer (with an accuracy of $\pm 2\%$ or $\pm$ 0.1 m/s) placed downstream of the plate. The flow Reynolds number Re (based on plate length) in the test is less than the critical Reynolds number Re_c of 10^5 for laminar-turbulent transition, which is considered appropriate for frost surfaces which are endowed with surface roughness [9]. Laminar flow is thus assumed throughout the frost growth period.

The air humidity is measured near the test section by Omega Model RH411/Thermo Hygrometer, whose accuracy is $\pm 3\%$. The room temperature is measured by the same instrument with an accuracy of $\pm$ 1 K). The variation in the relative humidity near the test section is achieved (controlled) primarily by opening the doors of the laboratory near the test section, but we also turned off the air-conditioning in that area as well, which helped to increase the humidity.

The frost thickness on the plate, which is nearly uniform, is measured at five locations (TC1 through TC5) located on the plate as shown (**Fig.** 2b), the TC5 being in the center of the plate. A precision vernier gauge with a dial caliper (accuracy of 0.127 mm) is used for measuring the frost thickness. Frost density is directly measured gravimetrically at three intermediate points of time. The frost density is also theoretically predicted with an extension of the model of [8]. The accuracy of the measured frost density is estimated to be about 20 kg/m^3.

During the initial cooling of the plate (when the plate surface temperature decreases from its initial room temperature value), the test plate is covered with a plastic film so that no frost is deposited on the plate surface. Once the plate reaches a steady state temperature, the plastic film is removed and frost measurements are commenced. The tests are carried out up to about 225-250 min. For safety purposes, oxygen concentration levels near the test area are monitored.

3 Frost Model Description

The experimental data obtained here are compared with an extension of the author's theoretical model [8]. Only the final results of the model that are directly relevant to the present investigation are presented as follows. The frost growth x_s, frost density ρ_f, and frost surface temperature T_s are shown to be expressed by

$$\frac{dx_s}{dt} = \frac{h_m(\omega_a - \omega_s)}{\rho_f\left\{1 + x_s\left[c_2\left(1-\xi^{0.5}\right)+\frac{1}{\theta}\right]\frac{1}{(T_m - T_w)}\frac{dT_{fs}}{dx_s}\right\}} \tag{1}$$

$$\frac{\rho_f}{\rho_{\text{ice}}} = 0.5\theta\exp\left\{-\left[c_1 + c_2(1-\theta)\right]\left(1-\xi^{0.5}\right)\right\} \tag{2}$$

$$T_s = T_w + \left(\frac{x_s}{k_f}\right)h_c(T_a - T_s) + \frac{1}{2}\left(\frac{x_s L_{sv}}{k_f}\right)\left[h_m(\omega_a - \omega_s) + \rho_f\frac{dx_s}{dt}\right] \tag{3}$$

where

$$\theta = (T_{fs} - T_w)/(T_m - T_w), \qquad \xi = \text{Re}/\text{Re}_c, \quad c_1 = 0.376, \quad c_2 = 1.5 \tag{4}$$

In the preceding equations, t denotes the time, T_w the wall temperature, h_c and h_m the convective heat and mass transfer coefficients respectively, T_a and T_m the air temperature and the melting temperatures respectively, ω_a and ω_s the humidity ratios at air temperature and at the frost surface temperature respectively, θ the dimensionless frost surface temperature, L_{sv} the latent heat of sublimation, ρ_{ice} the density of ice and Re_c the critical Reynolds number for laminar-turbulent transition. The Reynolds number is defined by

$$\text{Re} = uL/\nu \tag{5}$$

where u is the air velocity, L the characteristic plate length, and ν the kinematic viscosity of air.

This one-dimensional model is based on the work of Jones and Parker [1] and Cheng and Cheng [10]. It incorporates the water frost density correlation presented in [9]. The frost thermal conductivity model is taken from [11], which is based on the point contact model of Zehner and Schlunder [12,13], and regards the frost as made up of cylindrical particles. The Zehner-Schlunder model is known to be appropriate for the frost circumstances which involve ice to air conductivity ratio (of about 100) is less than 1000 [13,14]. This frost growth model [8] was validated with existing data for conditions of constant humidity.

The preceding model is extended in a straightforward manner to accommodate variable humidity by considering

$$\omega_a = \omega_a(t) \tag{6}$$

in Eqs. (1) and (2). The humidity ratio ω_s of course changes with time even for constant air humidity, since the frost surface temperature necessarily changes with time.

4. Results and Discussion

4.1. Constant Relative Humidity

Prior to validating the model [8] for the case of variable humidity, comparisons are first made between the model and the present data (Run #1) for constant relative humidity (**Fig.** 3). The data correspond to T_w = 263.7 K, T_a =295.1 K, ϕ_a =71.6%, and u_a =1.77 m/s. The flow Reynolds number based on the plate length is about $4x10^4$. It is seen from **Fig.** 3a that the data for frost thickness for the locations TC1 through TC5 are essentially uniform up to about 60 min. However, there is observed some non-uniformity in the frost thickness for the period between 100 and 150 min. Good agreement is noticed between the model and the data for up to about 60 min, considering that the frost thickness is less than 2 mm with the measured uncertainty of 0.127 mm. Note that the first data point corresponds to a frost thickness of about 0.75 mm. Beyond about 75 min, the theory is seen to underestimate the frost thickness.

Figure 3b shows a comparison of frost density predicted by the model with the test data taken at three instances in time. The overall agreement between the theory and the data for the frost density appears satisfactory. The predicted frost surface temperature (Eq. 3) at the end of the run (about 240 min) is about 271.4 K (a couple of degrees less than the freezing temperature of 273 K). The frost surface temperature is not the average temperature of the air flow, but represents the frost-air interface temperature. These comparisons serve to further validate the model for conditions of constant relative humidity.

4.2 Variable Relative Humidity

4.2.1 Humidity range of 81-54%

Figure 4 presents a comparison of the frost predictions with the present data (Run #2) for variable humidity in the range of 81 to 54%. The variation of the relative humidity is sketched in

Fig. 4a. Other test conditions are T_w = 255.4 K, T_a=295.0 K, and u_a=1.71 m/s. The flow Reynolds number based on plate length is about 3.8×10^4. As indicated in **Fig.** 4a, the frost thickness data at various locations is essentially uniform up to about 50 min. There is some degree of non-uniformity noticed in the frost thickness beyond about 50 min. The theory somewhat underpredicts the measured value, and is generally satisfactory for the entire test duration.

Figure 4b illustrates the frost density comparison, suggesting that good agreement is achieved between the theory and the data. As seen from **Fig.** 4c, the predicted frost surface temperature at the end of the run (about 240 min) is about 267.7 K (less than the freezing temperature).

When compared to Run #1 (with constant relative humidity of 71.6%), the air temperature and the air velocity are nearly the same in both Runs #1 and #2. The average relative humidity in Run #2 for the test duration is about 67.5 % as compared to 71.6% for Run #1. The plate surface temperatures in the two sets of data differ by about 6 K (263.7 K for Run #1 and 255.4 K for Run #2). Thus it is seen that for Run #1 the plate temperature and the average relative humidity are larger relative to those of Run #2.

It is known that an increase in humidity increases the frost thickness, while an increase in plate temperature decreases the frost thickness [3]. It is also known that higher relative humidity leads to higher frost density. A direct comparison of the data of Run #1 and Run #2 for frost thickness suggests that the frost thickness is greater and frost density is smaller in Run #2 compared to Run #1. It is evident that the influence of decreased wall temperature more than offsets the effect due to a decrease in relative humidity, so that the combined effect produces a greater frost thickness in the case of Run #2 relative to Run #1.

The relationship between relative humidity, frost thickness, and frost density is not as simple as expressed above. We also need to consider how the relative humidity contributes to the porous structure and possible ice layer growth on the top of the aluminum plate.

4.2.1 Humidity range of 66-59%

Figure 5 shows a comparison of the present data (Run #3) for variable humidity in the range of 66-59%. The variation of the relative humidity is presented in **Fig.** 5a. Other test conditions are T_w = 255.4 K, T_a =291.8 K, and u_a =2.44 m/s. Thus the wall temperature is the same as in Run #2. The flow Reynolds number based on the plate length is about 5×10^4. It is noticed from

Fig. 5b that the measured frost thickness appears essentially uniform up to about 50 min (as in the case of Run #2, **Fig.** 4b). Some degree of nonuniformity in the frost thickness is evident beyond 50 min. The theory begins to deviate from the measurements at about 15 min, and somewhat underpredicts the data. In general the model for the variable humidity is again reasonably satisfactory.

The density comparisons in this case were only made at two points in time. The theory underpredicts the data, and is not as satisfactory as is observed in the case of Run #2. **Fig.** 5c suggests that the predicted frost surface temperature at the end of the run (about 230 min) is about 267 K.

A direct comparison of the results for Run #2 and Run #3 reveals that at a given time the measured frost thickness for Run #3 is less than that for Run #2. This is to be expected in view of higher relative humidity level for Run #2, and recognizing that the small change in the air velocity between the two runs has no appreciable effect on frost thickness [8].

It is true that the present data for variable humidity are restricted to a single wall temperature of 255.4 K. Data with variable wall temperatures would be valuable in further validating the model. In view of the difficulties associated with maintaining a constant wall temperature with the aid of the solenoid valve, additional data could not be obtained at other wall temperatures. Also the density data could be obtained at larger points in time. Finally, the system needs improvement to accurately measure all parameters related to the frost thickness and density, such as frost surface temperature and heat flux. In view of these considerations, the data presented here should only be considered preliminary in our attempts to experimentally and theoretically investigate frost formation under conditions of variable humidity.

5. Conclusions

The comparison of the author's frost model [8] with the present data reveals that the theory satisfactorily describes the frost growth and densification for the conditions of constant as well as variable humidity with regard to laminar flow over flat surfaces. It is concluded that the frost models developed for constant humidity may be directly applied to circumstances of variable humidity. It is hoped that frost data for variable wall temperature will become available so that frost models for arbitrary wall temperature can be validated.

Acknowledgments

The author would like to thank Brian Hunter and Kevin Jumper at the Cryogenics Laboratory at NASA Kennedy Space Center with regard to experimental test support. This work was funded by NASA Kennedy Space Center, with mark Collard as Project Manager. Thanks are also due to Stanley Starr (Chief, Applied Physics Branch) of NASA Kennedy Space Center for review and helpful suggestions.

References

[1] B.W. Jones, J.D. Parker, Frost formation with varying environmental parameters, J. Heat Transfer 97 (1975) 255-259.

[2] J.D. Yonko, C.F. Sepsy, An investigation of the thermal conductivity of frost while forming on a flat horizontal plate, ASHRAE Trans. 73 (part 1) (1967) 1.1-1.11 (Paper No. 2043).

[3] R. Östin, R.S. Anderson, Frost growth parameters in a forced air stream, International Journal of Heat Mass Transfer 34 (4/5) (1991) 1009-1017.

[4] K-S Lee, W.S. Kim, T.H. Lee, A one-dimensional model for frost formation on a cold flat surface, International Journal of Heat and Mass Transfer 40 (18) (1997) 4359-4365.

[5] K-S Lee, S. Jhee, D-K Yang, Prediction of the frost formation on a cold flat surface, International Journal of Heat and Mass Transfer 46 (2003) 3789-3796.

[6] C-H Cheng, K-K Wu, Observations of early-stage frost formation on a cold plate in atmospheric air flow, Journal of Heat Transfer 125 (2003) 95-102.

[7] C.J.L. Hermes, R.O. Picucco, J.R. Barbosa, Jr., C. Melo, A study of frost growth and densification on flat surfaces, Experimental Thermal Fluid Sciences 33 (2009) 371-379.

[8] M. Kandula, Frost growth and densification in laminar flow over flat surfaces, International Journal of Heat Mass transfer 54 (2011) 3719-3731.

[9] M. Kandula, Correlation of water frost porosity in laminar flow over flat surfaces, Special Topics and Reviews in Porous Media 3 (1) (2012) 79-87.

[10] C.-H. Cheng, Y.-C. Cheng, Predictions of frost growth on a cold plate in atmospheric air, International Communications in Heat Mass Transfer 28 (7) (2001) 953-962.

[11] M. Kandula, Effective thermal conductivity of frost considering mass diffusion and eddy convection, Special Topics and Reviews in Porous Media 1 (4) (2010) 321-336.

[12] P. Zehner, P., E.U. Schlunder, Thermal conductivity of granular materials at moderate temperatures Chemie Ingr. Tech. 42 (1970) 933-941 (in German).

[13] C.T. Hsu, P. Cheng, P., K.W. Wong, Modified Zehner-Schlunder models for stagnant thermal conductivity of porous media, International Journal of Heat Mass Transfer 37 (17) (1994) 2751-2759.

[14] M. Kandula, On the effective thermal conductivity of porous packed beds with uniform spherical particles, Journal of Porous Media 14 (2010) 919-926.

Figure Captions

Fig. 1. Schematic of the experimental setup.

Fig. 2. Photographic views of the experimental facility.

Fig. 3. Comparisons of frost thickness and frost density for Run #1 with constant relative humidity.

Fig. 4. Comparisons for Run #2 with variable relative humidity.

Fig. 5. Comparisons for Run #3 with variable relative humidity.

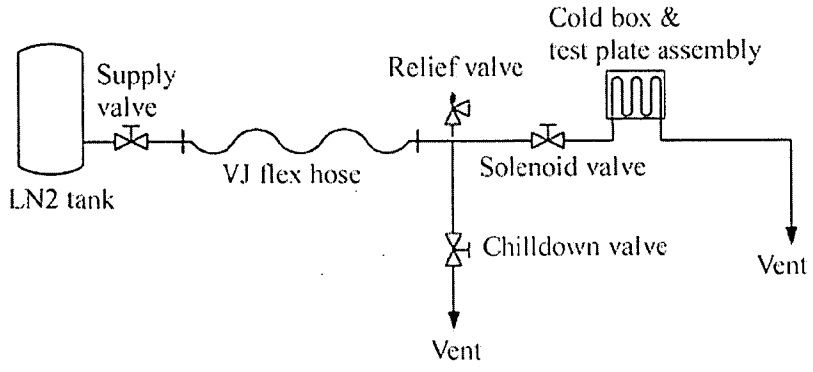

Fig. 1. Schematic of the experimental setup.

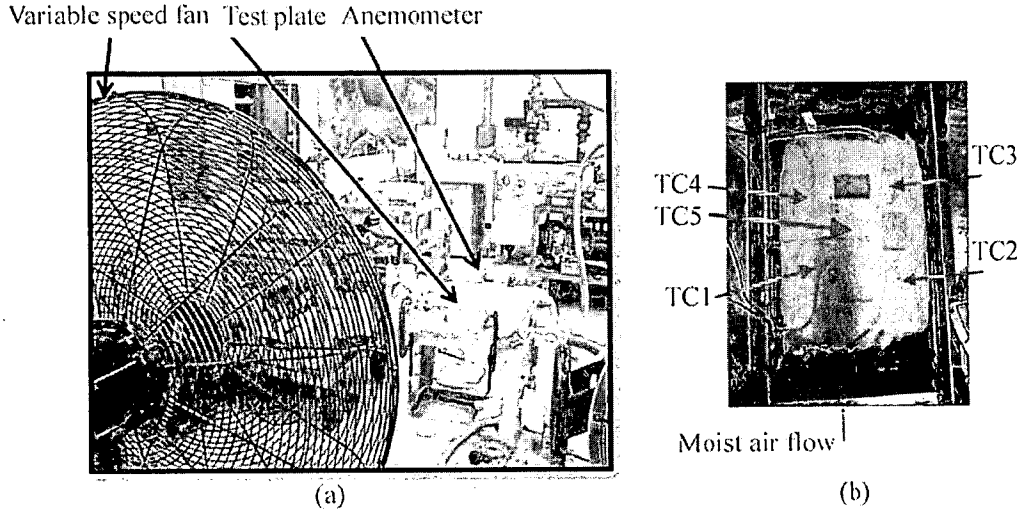

Fig. 2. Photographic views of the experimental facility.

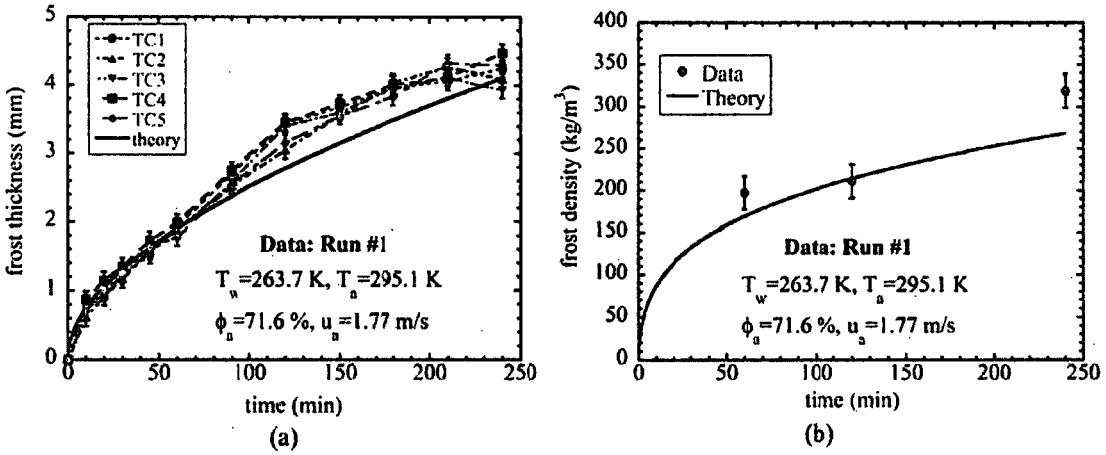

Fig. 3. Comparisons of frost thickness and frost density for Run #1 with constant relative humidity.

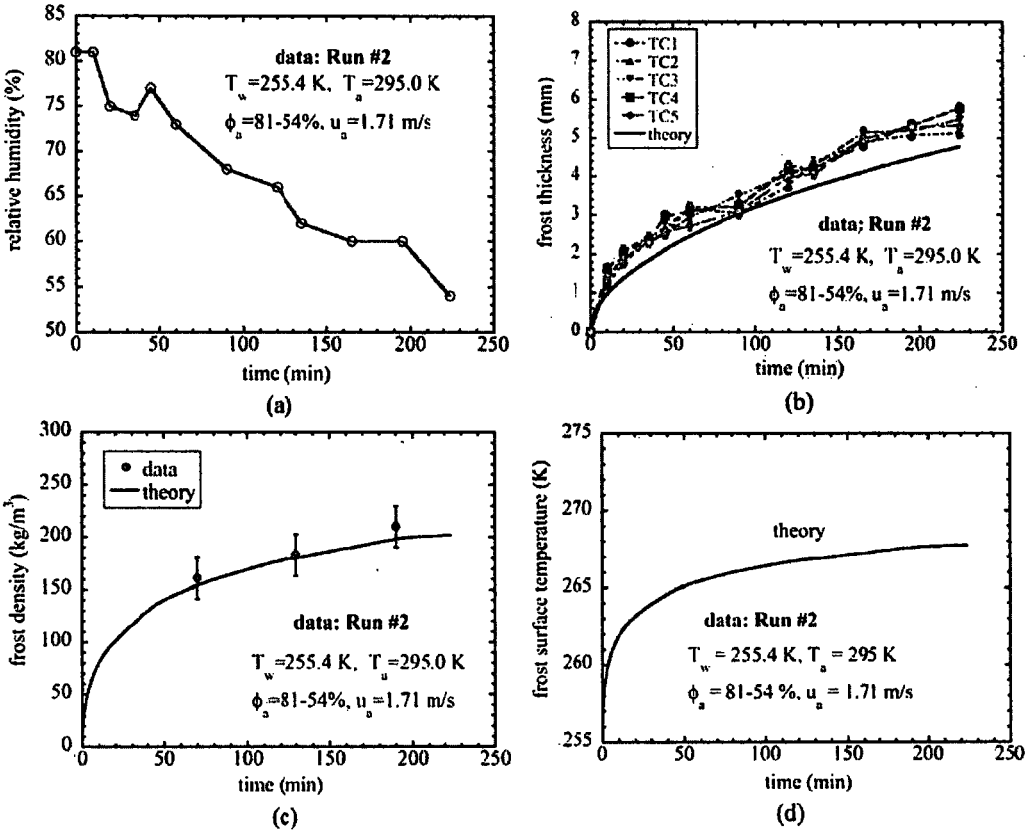

Fig. 4. Comparisons for Run #2 with variable relative humidity.

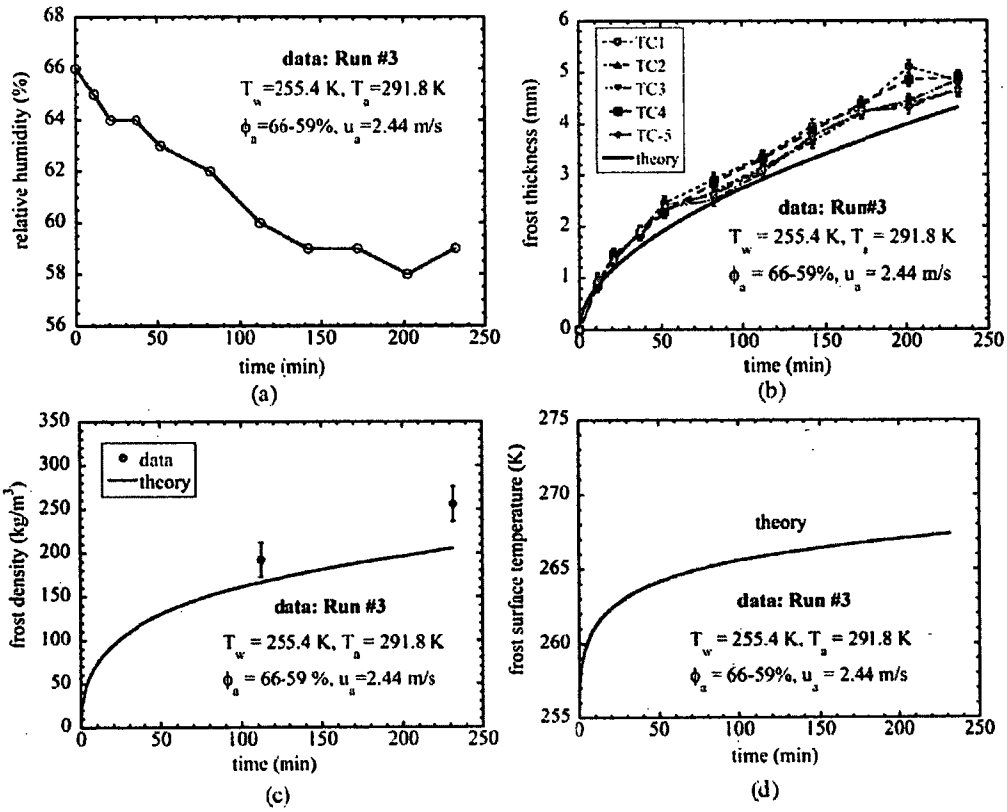

Fig. 5. Comparisons for Run #3 with variable relative humidity.